Supplementary Information

Low Compressibility of Photoelectric Properties in the Layered Molecular Non-Metal Halide AsI_3

Zonglun Li[a,b,c], Dexiang Gao[a,b], Shuxin Chen[c], Lei Yue[c], Bao Yuan[a,b], Xudong Shen[a,b], Le Kang[a,b,], Quanjun Li[c,*], Bingbing Liu[c]*

[a]Institute of High Energy Physics, Chinese Academy of Sciences, Beijing 100049, China
[b]Spallation Neutron Source Science Center, Dongguan 523803, China.
[c]State Key Laboratory of High Pressure and Superhard Materials, Jilin University, Changchun 130012, China.

*Correspondence and requests for materials should be addressed to L.K. (email: kangl@ihep.ac.cn), or to Q.J.L. (email: liquanjun@jlu.edu.cn)

Key words: AsI_3, photoelectric properties, high pressure, molecular crystal, compressibility

S1: Crystal structure of AsI_3 at ambient conditions.

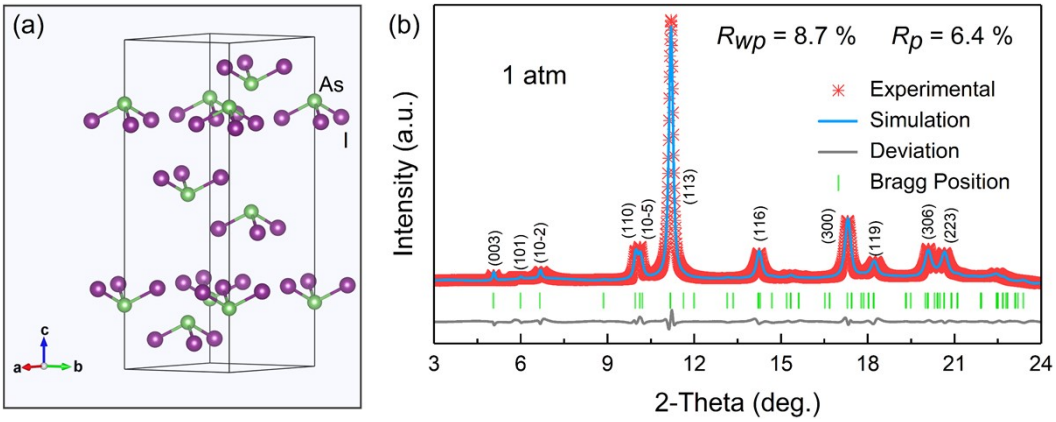

Fig. S1. (a) Crystal structure of $R\bar{3}$ phase AsI_3 at ambient conditions. (b) Rietveld refinements result of $R\bar{3}$ phase AsI_3 at ambient conditions.

S2: Evolution in synchrotron XRD patterns of AsI_3 under high pressure.

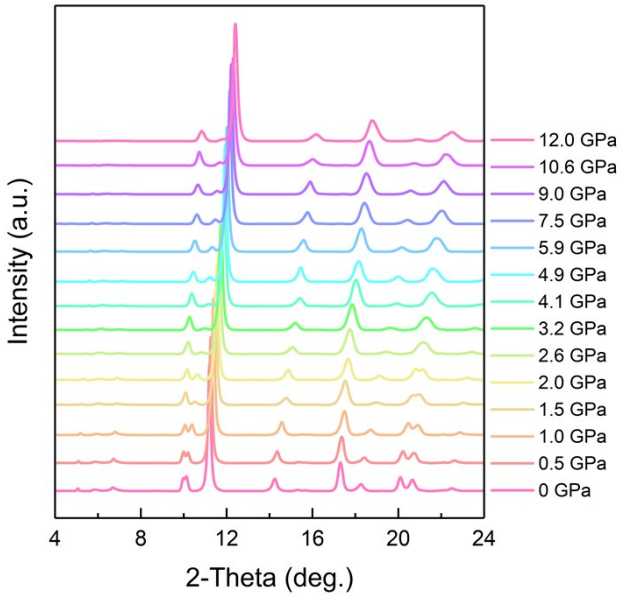

Fig. S2. Synchrotron X-ray diffraction (XRD) patterns of AsI_3 powders at selected pressures.

S3: Compressibility of AsI_3.

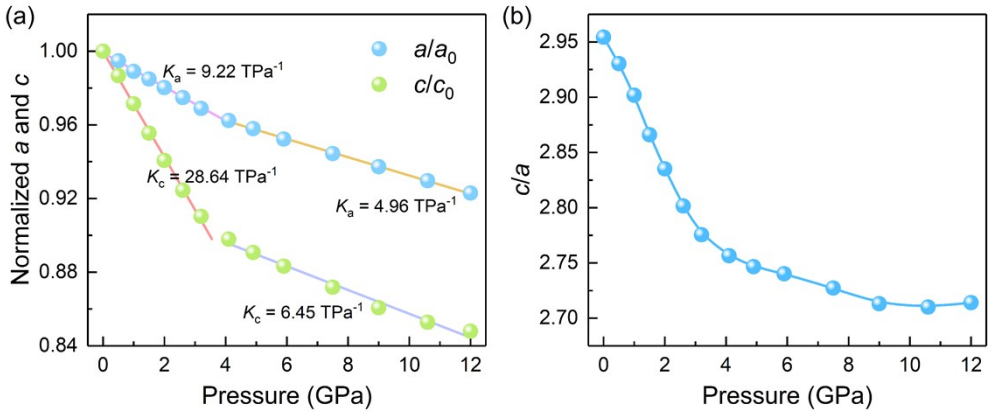

Fig. S3. (a) Evolution of the normalized cell parameters a/a_0 and c/c_0 of AsI_3 as a function of pressure. (b) Evolution of the ratio of c/a of AsI_3 as a function of pressure.

S4: Rietveld refinement results of AsI_3 at various pressures.

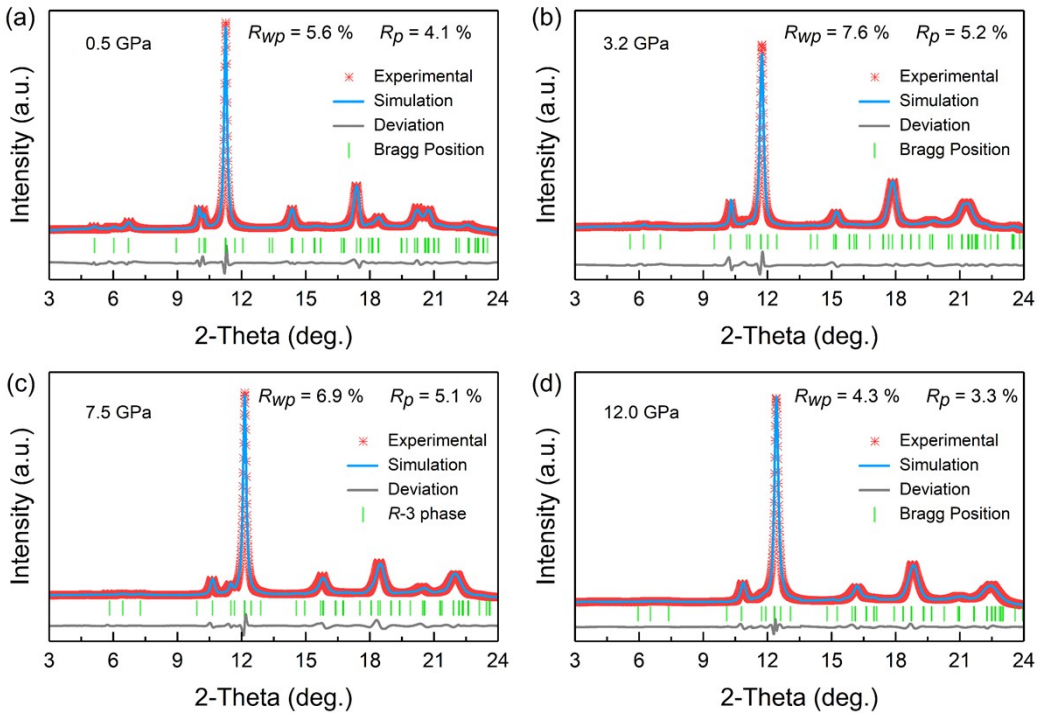

Fig. S4. Rietveld refinements results of AsI_3 under various pressures. (a) 0.5 GPa. (b) 3.2 GPa. (c) 7.5 GPa. (d) 12.0 GPa.

S5: Lattice dynamics of AsI_3 at ambient conditions.

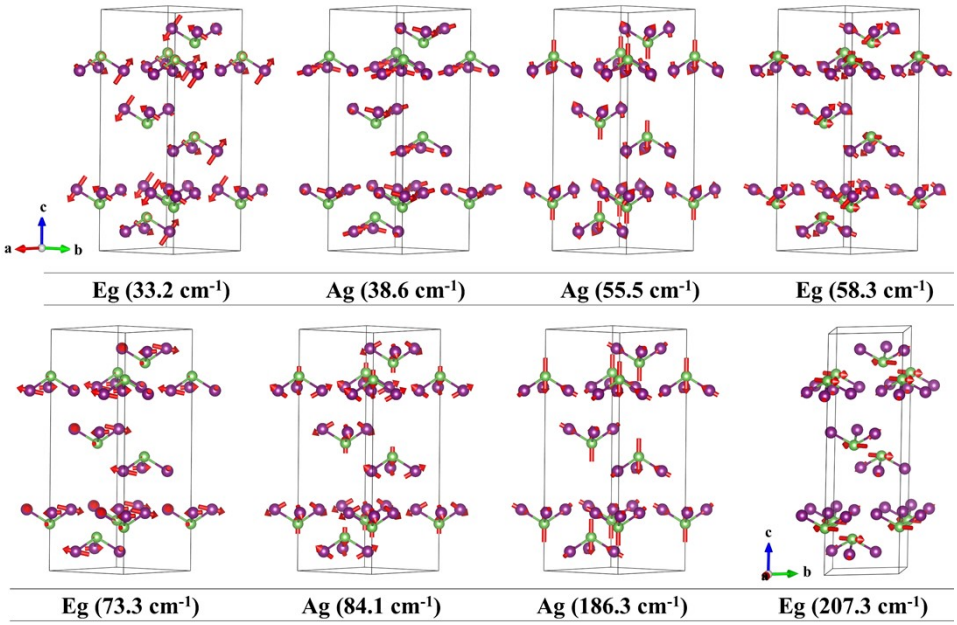

Fig. S5. Calculated vibrational patterns for the most prominent Raman modes of AsI_3 at ambient conditions. The vibration frequencies are shown at the bottom of each pattern. Raman vibration modes were calculated using density functional perturbation theory (DFPT)[1, 2] as implemented in the Phonopy package[3, 4] and visualized using the VESTA package.[5] Furthermore, the E_g mode at 58.3 cm^{-1} is difficult to observe at ambient temperatures and can be detected at low temperatures.[6] We also failed to recognize this mode, so vibrational patterns of Eg at 58.3cm^{-1} can be used as a reference here.

S6: The crystal orbital Hamilton population (COHP) analysis.

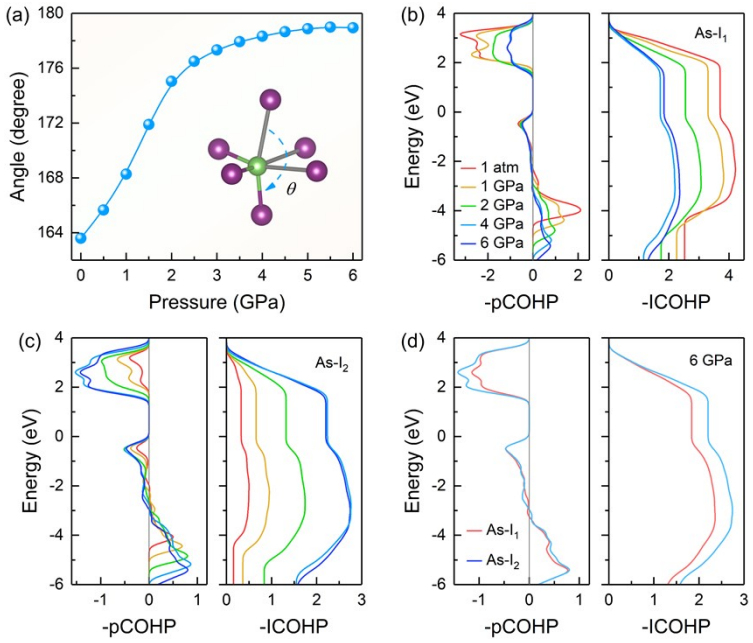

Fig. S6. (a) The calculated I-As-I angle of AsI_3 as a function of pressure. (b-c) The negative crystal orbital Hamilton population (-COHP) and the negative integrated COHP (-ICOHP) of As-I_1 and As-I_2 bonds in AsI_3 at selected pressures. (d) The -COHP and -ICOHP of As-I_1 and As-I_2 bonds at 6 GPa. The crystal orbital Hamilton population (COHP) was calculated by using the plane wave methods as implemented in the LOBSTER package.[7, 8]

S7. Photocurrent response at selected external bias.

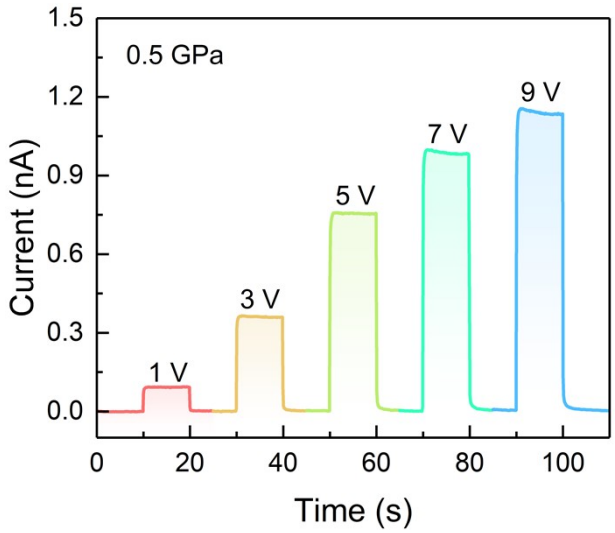

Fig. S7. The photocurrent curves of AsI_3 under 520 nm laser illumination at external bias from 1 to 9 V.

S8. Photocurrent with 520 nm laser illumination under high pressure.

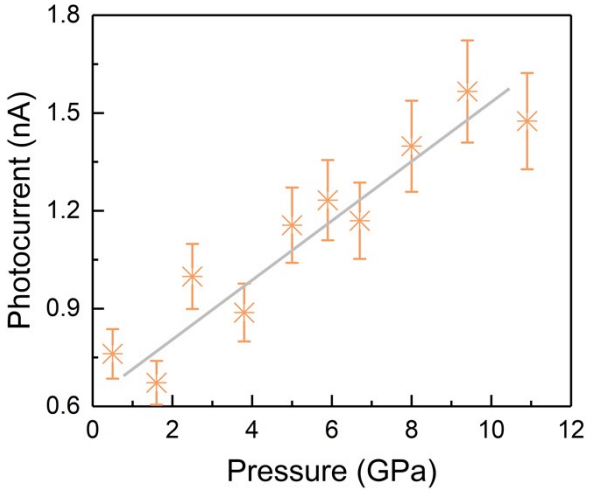

Fig. S8. Changes in the photocurrent of the AsI_3 device when illuminated with a 520 nm laser at various pressures.

S9. 2D band structure of AsI_3 at selected pressures.

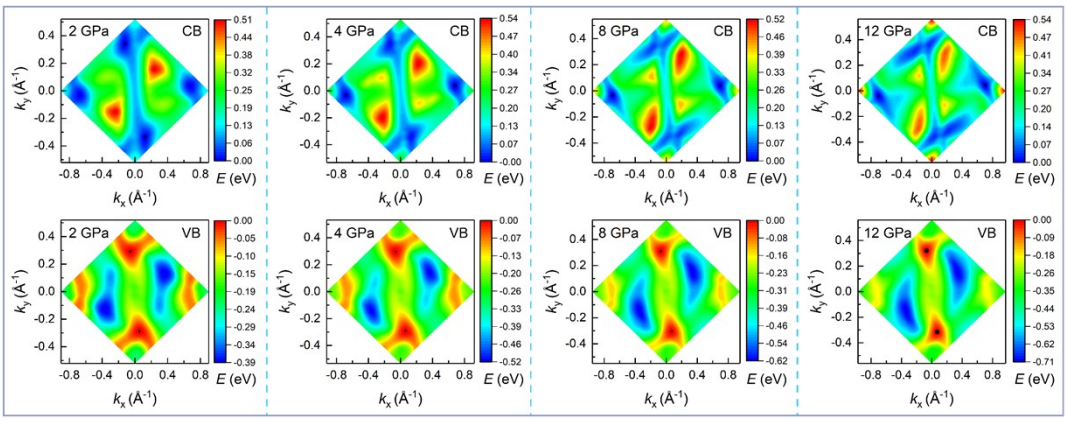

Fig. S9. 2D projections of the valence bands (VB) and conduction bands (CB) of AsI_3 in the first Brillouin zone at selected pressures. The black circle indicates the VBM or the CBM.

S10. Partial density of states for various layered iodides.

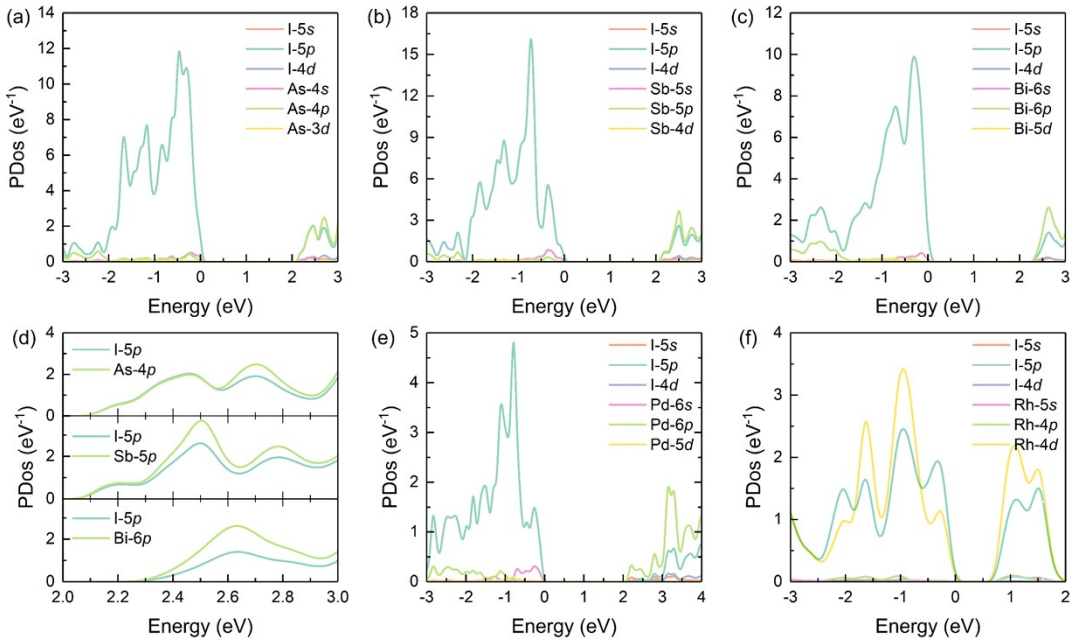

Fig. S10. Partial density of states for various layered iodides at ambient pressure. (a) AsI_3, (b) SbI_3, (c)BiI_3, (d) Zoomed-in partial density of states for the conduction bands of AsI_3, SbI_3, and BiI_3. (e) PbI_2, and (f) RhI_3.

S11. Partial density of states for various non-layered metal iodides.

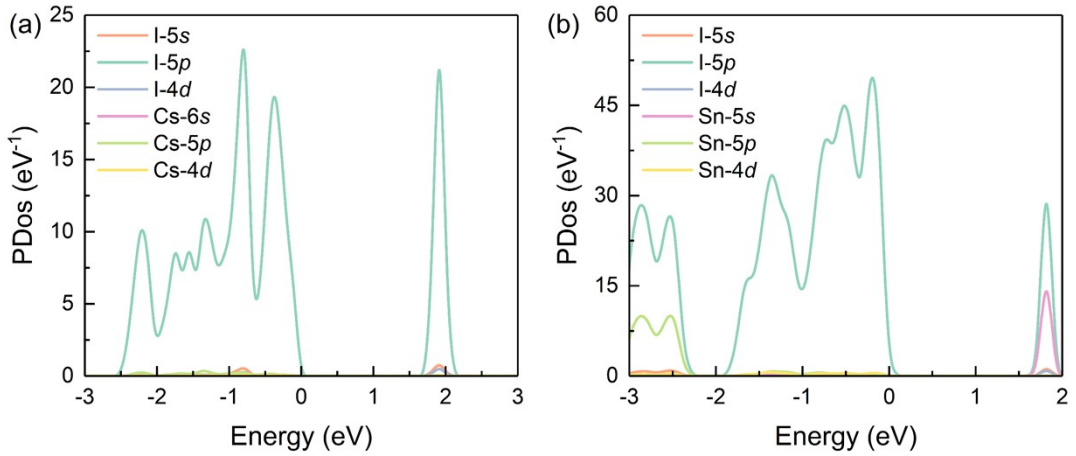

Fig. S11. Partial density of states for various non-layered metal iodides at ambient pressure, (a) CsI_3, (b) SnI_4.

S12. Partial charge density and photocurrent in non-layered metal iodides.

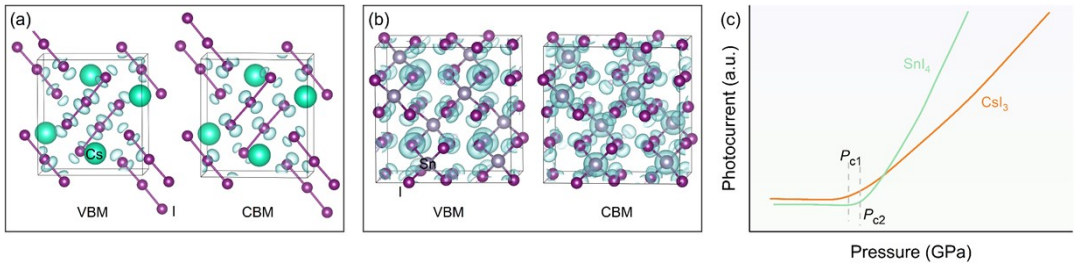

Fig. S12. Charge distribution of the VBM and CBM of non-layered metal iodides at ambient pressure, (a) CsI_3,[9] (b) SnI_4.[10] (c) Schematic diagram illustrating variations in the photocurrent response of CsI_3 and SnI_4 under high pressure.

S13. Phonon dispersion curve of AsI_3 at ambient pressure.

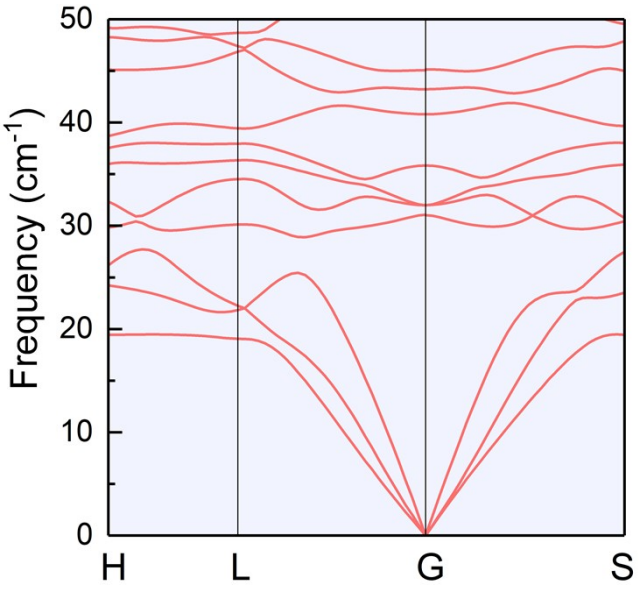

Fig. S13. (a) Phonon dispersion curve of AsI_3 at ambient pressure. The phonon spectra were obtained by employing the CASTEP package[11, 12], which demonstrates the rationality and reliability of the structural optimization.

References

1. P. Giannozzi, S. de Gironcoli, P. Pavone and S. Baroni, *Phys. Rev. B*, 1991, **43**, 7231-7242.
2. X. Gonze and C. Lee, *Phys. Rev. B*, 1997, **55**, 10355-10368.
3. A. Togo, L. Chaput, T. Tadano and I. Tanaka, *J. Phys.: Condens. Matter*, 2023, **35**, 353001.
4. A. Togo, *J. Phys. Soc. Jpn.*, 2022, **92**, 012001.
5. K. Momma and F. Izumi, *J.Appl.Cryst.*, 2011, **44**, 1272-1276.
6. H. C. Hsueh, R. K. Chen, H. Vass, S. J. Clark, G. J. Ackland, W. C. K. Poon and J. Crain, *Phys. Rev. B*, 1998, **58**, 14812-14822.
7. R. Dronskowski and P. E. Bloechl, *J. Phys. Chem.*, 1993, **97**, 8617-8624.
8. A. Decker, G. A. Landrum and R. Dronskowski, *Z. anorg. allg. Chem.*, 2002, **628**, 295-302.
9. Z. Li, Q. Li, H. Li, L. Yue, D. Zhao, F. Tian, Q. Dong, X. Zhang, X. Jin, L. Zhang, R. Liu and B. Liu, *Adv. Funct. Mater.*, 2022, **32**, 2108636.
10. R. Lu, Z. Li, L. Yue, L. Song, S. Fang, T. Liu, P. Shen, Q. Li, X. Jin and B. Liu, *Mater. Today Phys.*, 2024, **42**, 101381.
11. S. J. Clark, M. D. Segall, C. J. Pickard, P. J. Hasnip, M. I. J. Probert, K. Refson and M. C. Payne, *Z. Krist.*, 2005, **220**, 567-570.
12. K. Refson, P. R. Tulip and S. J. Clark, *Phys. Rev. B*, 2006, **73**, 155114.